Negative electron affinity from aluminium on the diamond (1 0 0) surface: a theoretical study

IOP Publishing Journal of Physics: Condensed Matter
J. Phys.: Condens. Matter **30** (2018) 235002 (9pp) https://doi.org/10.1088/1361-648X/aac041

Negative electron affinity from aluminium on the diamond (1 0 0) surface: a theoretical study

Michael C James[1,2], Alex Croot[3], Paul W May[1] and Neil L Allan[1]

[1] School of Chemistry, University of Bristol, Cantock's Close, Bristol BS8 1TS, United Kingdom
[2] Bristol Centre for Functional Nanomaterials, HH Wills Physics Laboratory, University of Bristol, Tyndall Avenue, Bristol BS8 1TL, United Kingdom
[3] School of Physics, HH Wills Physics Laboratory, University of Bristol, Tyndall Avenue, BS8 1TL, United Kingdom

E-mail: michael.james@bristol.ac.uk

Received 22 March 2018, revised 17 April 2018
Accepted for publication 26 April 2018
Published 15 May 2018

Abstract

Density functional theory calculations were performed to model the adsorption of up to 1 monolayer (ML) of aluminium on the bare and O-terminated (1 0 0) diamond surface. Large adsorption energies of up to −6.36 eV per atom are observed for the Al-adsorbed O-terminated diamond surface. Most adsorption sites give a negative electron affinity (NEA), with the largest NEAs −1.47 eV on the bare surface (1 ML coverage) and −1.36 eV on the O-terminated surface (0.25 ML coverage). The associated adsorption energies per Al atom for these sites are −4.11 eV and −5.24 eV, respectively. Thus, with suitably controlled coverage, Al on diamond shows promise as a thermally-stable surface for electron emission applications.

Keywords: diamond, DFT, negative electron affinity, surface

(Some figures may appear in colour only in the online journal)

Introduction

The desirable bulk properties of diamond, coupled with its ability to form a negative electron affinity (NEA) surface is of technological interest for numerous electron emission applications including photodiodes [1], electron sources [2], secondary electron emission [3] and renewable energy generation [4]. Furthermore, low work function diamond devices have potential for surface transfer doping applications [5]. In a material with an NEA, the conduction band minimum (CBM) is higher in energy than the surrounding vacuum, leading to virtually barrierless electron emission when electrons are excited into the conduction band (figure 1). To form an NEA material, it is necessary to terminate the surface with atoms or groups of atoms that are electropositive relative to the bulk material, forming an electric dipole perpendicular to the surface with positive charge outermost. For diamond, simple H termination gives an NEA for each of the (1 0 0), (1 1 1) and (1 1 0) surfaces [6–8]. However, H-terminated diamond surfaces suffer from hydrogen desorption at elevated temperatures (≳700 °C) [9]. This makes H-terminated diamond unsuitable for high-temperature applications, such as thermionic energy converters [4], and so there is an extensive search for alternatives with which to terminate diamond that provide high NEA whilst remaining stable at thermionic operating temperatures.

Previous experimental and computational studies of NEA surfaces on diamond include the use of group I and II metals [10–13] and first-row transition metals (TMs) [14–19] as the electropositive species, with monolayer or sub-monolayer coverage on bare or oxidised diamond surfaces. Group I elements have long been known to exhibit NEA characteristics on diamond, but larger adsorbed group I elements have low thermal stability which limits their usefulness at higher temperatures. For example, despite an extremely low work function of ~1.5 eV, the CsO-terminated diamond surface loses Cs through desorption, and so the NEA is lost above ~400 °C [10]. Thus, recent computational and experimental work has concentrated on elements that can provide a more

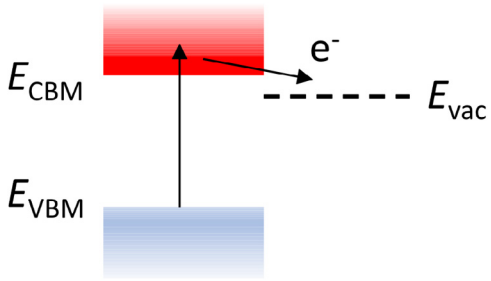

Figure 1. NEA arises when the conduction band minimum (CBM) is higher in energy than the surrounding vacuum. Electrons in the valence band, with a maximum energy at the valence band maximum (VBM) of E_{VBM}, are excited into the conduction band by photon absorption, thermal collisions or electric fields.

robust surface in addition to NEA, focusing on small group I and II metals, such as Li and Mg [20–22]. Experimental work with certain TMs shows NEA emerges from deposition of thin (<10 Å) layers onto bare or oxidised diamond surfaces [14–17]. The magnitude of the NEA varies with the TM and layer thickness. Computational work has also predicted NEA with various first-row TMs, including Cu, Ni, Ti and Zn, on both bare and O-terminated diamond surfaces, with results suggesting that carbide-forming TMs give a larger NEA [18, 23].

Aluminium on the diamond surface has thus far been omitted from NEA studies, even though Al forms a carbide and bonds sufficiently well to a diamond surface to act as either Ohmic or Schottky contacts for diamond-based devices [24]. Al_2O_3 on diamond is a candidate material for device interfaces in MOSFETs [25] and MOSCAPs [26] and additionally for passivation of the p-type conductive surface found on H-terminated diamond that results from surface transfer doping [27]. However, these are typically thicker films than what is required to give NEA. In this work we show that up to 1 ML of aluminium on bare and O-terminated diamond has considerable potential for NEA devices.

Method

Plane-wave density functional theory (DFT) calculations were carried out using the Cambridge Serial Total Energy Package (CASTEP) code [28]. The diamond slab consisted of 14 carbon layers, sufficient to represent bulk diamond at the centre. The slab is periodic in the x and y directions and terminated on both sides by a 2×2 supercell of the (1 0 0) surface. The slab width was fixed at 5.05 Å × 5.05 Å with a vacuum gap of 20–25 Å separating repeating slabs, chosen such that the electrostatic potential had fully decayed in the vacuum. A basis set of plane waves with an energy cut-off of 700 eV, the Perdew–Burke–Ernzerhof (PBE) generalised gradient approximation (GGA) for the exchange-correlation functional [29] and Vanderbilt pseudopotentials [30] were used in all calculations. Density-of-states calculations were calculated using the OptaDOS code [31] with adaptive broadening and DOS spacing of 0.07 eV. The Brillouin zone was sampled by a $6 \times 6 \times 1$ Monkhorst–Pack k-point grid [32] for energy minimisation steps and a $12 \times 12 \times 1$ k-point grid for DOS calculations. The energy of the slab was minimised with respect to all atomic positions. The tolerances for convergence of ionic forces and total energy were 0.05 eV Å^{-1} and 2×10^{-5} eV/atom, respectively.

The ionisation energy I was calculated using the method of Fall *et al* [33], shown in equation (1) as the difference between vacuum and valence band maximum (VBM) energies. The electron affinity (EA) χ is calculated by subtraction of the experimental band gap, E_g, from the ionisation energy, as shown in equation (2).

$$I = E_{vac} - E_{VBM} = E_{vac} - (V_{slab} + E_{VBM,bulk} - V_{bulk}) \quad (1)$$

$$\chi = I - E_g. \quad (2)$$

E_{vac} is the energy of the vacuum level, E_{VBM} the valence band maximum, V_{slab} the average slab potential, $E_{VBM,\ bulk}$ the valence band maximum calculated for bulk diamond, and V_{bulk} the average potential energy in the bulk. The difference between $E_{VBM,\ bulk}$ and V_{bulk} has been calculated previously [34]. The experimental value of the band gap, E_g, of 5.47 eV was used because the GGA method underestimates the band gap of diamond [18].

The energy of adsorption E_{ads} was calculated from the energy of the structure containing both diamond slab and adsorbates E_{total} by subtraction of the diamond slab energy E_{slab} with no adsorbate, and the energy of an isolated adsorbate atom E_{at} multiplied by the number of adsorbate atoms N. This divided by the total number of adsorbate atoms gives the energy per adsorbate (equation (3)). A negative E_{ads} indicates exothermic adsorption.

$$E_{ads} = (E_{total} - E_{slab} - NE_{at})/N. \quad (3)$$

For validation purposes, calculations were initially performed on the bare, H- and O-terminated diamond surfaces, and compared with previous published calculations. Table 1 shows that calculated energies and bond lengths are in good agreement with previous work. Values for adsorption energies are the most variable as they are particularly sensitive to the computational parameters, such as functionals used and the basis set. For diamond, DFT calculations generally give larger electron affinities than those measured experimentally [35]. This is related not only to the approximations in the DFT method, but also uncertainty in the surface coverages achieved experimentally.

Geometry optimisation

In this work, we define one atom per surface unit cell as constituting a monolayer (ML), and thus four atoms constitute 1 ML of the 2×2 supercell used here to represent the diamond surface. Both the bare and the oxygen-terminated surface were considered.

Al addition to the bare diamond surface

Upon geometry optimisation, the bare diamond surface reconstructs to a (2×1) arrangement, forming dimer rows on the surface (figure 2). Between 1 and 4 Al atoms were added to both sides of the relaxed bare diamond slab, each atom

Table 1. Values of the adsorption energy, E_{ads}, calculated electron affinity, χ, and bond lengths, d, for selected calculations compared with previous works. d(C–C) refers to bond length of the surface dimer. (2 × 1) indicates a reconstructed surface dimer. The two O-terminations are discussed in further detail in the main text.

Structure	Source	E_{ads} (eV)	χ (eV)	d(C–C) (Å)	d(C–O) (Å)	d(C–H) (Å)
C(100)-(2 × 1)	Previous calculations	−1.46 [34], −1.512 [36]	0.51–0.69 [37], 0.62 [34], 0.8 [6] 0.28 [38]	1.38 [34], 1.37 [39]	—	—
	Current work	−1.60[a]	0.53	1.38	—	—
C(100)-(2 × 1):2 H	Previous calculations	−5.32 [34], −4.54 [39]	−1.95 [34], −2 [37], −2.2 [6]	1.62 [34], 1.61 [39]	—	1.1 [34, 39]
	Current work	−4.14	−2.06	1.62	—	1.1
C(100)-(1 × 1):O (ether)	Previous calculations	−8.2 [34], −8.43 [40]	2.61–2.7 [40], 2.63 [34]	—	1.5 [34], 1.49 [40], 1.48 [41]	—
	Current work	−7.47	2.54	—	1.5	—
C(100)-(1 × 1):O (ketone)	Previous calculations	−7.88 [34], −8.57 [40]	3.75 [34], 3.64 [40]	—	1.2 [34], 1.25 [40], 1.16 [41]	—
	Current work	−7.18	3.46	—	1.2	—

[a] Per surface atom, compared with the (1 × 1) bare surface.

representing 0.25 ML coverage. For the bare (2 × 1) reconstructed surface, four high-symmetry positions have been defined: the pedestal (HH), bridge (HB), valley bridge (T3) and cave (T4) sites (figure 2) [13]. Above 0.25 ML coverage, combinations of these sites are considered. For 0.5 ML coverage, Al atoms were positioned either in identical sites, representing rows perpendicular to the carbon dimer bonds, in pairs of sites parallel to the carbon dimer bonds for one half of the 2 × 2 supercell, or in a ($\sqrt{2} \times \sqrt{2}$) configuration where Al atoms are at diagonals to the supercell. For 1 ML coverage, Al atoms were in two sets of identical sites.

Table 2 displays the results for these surface arrangements for Al on the bare diamond surface, while the lowest energy positions for different surface coverages are shown in figure 3. For 0.25 and 0.5 ML coverage, the T4 site was found to be lowest in energy, while at 1 ML coverage the lowest energy configuration came from a parallelogram arrangement of Al atoms outside high symmetry sites, formed here by relaxation from the HH + T3 positions. This gave a hexagonal structure of Al atoms in the same plane, with Al–Al bond lengths of 2.52 Å in the *y* direction and 2.74–2.91 Å otherwise (figure 3(c)). This geometry is similar to that in the hexagonal (1 1 1) plane of bulk Al metal in which the Al–Al nearest neighbour distance is 2.86 Å; here Al–Al bonds are shorter because of epitaxial bonding of Al with the outermost carbon atoms.

The lengthening of the carbon dimer from 1.38 Å for the bare surface to between 1.63–1.85 Å suggests a change from a double to a very extended single bond. This is accompanied by a substantial reduction in Mulliken [42] bond population of the carbon dimer from 1.36 before Al addition to 0.52–0.78 after. The bond populations between Al and C atoms in the surface dimer lie between 0.02 and 0.67 and there is a correlation with the magnitude of the adsorption energies. Mulliken population analysis shows Al gains a positive charge of up to 0.9*e*, 0.8*e* and 0.4*e* for 0.25, 0.5 and 1 ML, respectively. The majority of negative charge is located on carbon atoms in the dimer row. There is a noticeable distinction between Al at the 4-coordinated HH and T3 sites and the 2-coordinated HB and T4 sites. The bonding at the 4-coordinate sites possess larger Mulliken charges but smaller Al–C_{dimer} Mulliken bond populations and so we define the 4-coordinate sites as 'ionic' and the 2-coordinate sites as 'covalent'. Al preferentially bonds to the 2-coordinate, more covalent sites, shown by larger E_{ads} values.

EA is strongly affected by the positioning of the Al atoms, with covalent sites showing more negative EA. Most sites show an NEA ranging from −0.1 to almost −1.5 eV, but for 0.5 ML both the linear and ($\sqrt{2} \times \sqrt{2}$) arrangement for the HH + T3 configuration have positive EA. Comparing Al with the TMs studied by Tiwari *et al* [18, 23] we find the EA of Al is, in general, more negative than those for Cu, Ni and V, and the variation with position smaller. Whilst they find Ti can possess a negative electron affinity larger than Al, for 0.5 and 1 ML coverages of Ti the most stable site has positive EA. Al has, generally, a larger adsorption energy than Cu, about the same as Ni, and smaller than V and Ti. The lowest energy adsorption sites for Al are different to these TMs—for

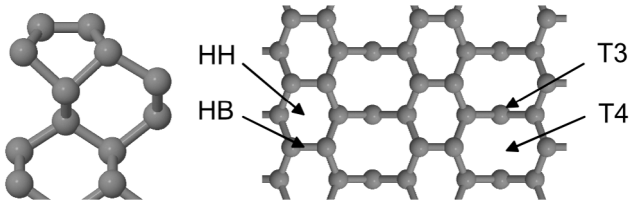

Figure 2. Side and plan view of the bare (2 × 1) reconstructed diamond surface. The plan view shows possible high symmetry sites for surface adsorbates.

the Al-adsorbed bare surface T4 (covalent) sites are preferred over T3 (ionic) sites at <1 ML coverages. It is also worth noting that overall the magnitude of the adsorption energies for Al are smaller than the adsorption energy for H on the bare surface (table 1).

Al addition to the O-terminated surface

The clean O-terminated surface has two possible low-energy configurations: the ether arrangement, where the oxygen bridges between two adjacent surface carbons, and the ketone arrangement, involving a C=O double bond normal to the surface (figure 4). These structures are similar in energy so both were considered for this study. In both cases, the unreconstructed (1 × 1) O-terminated surface has only two high-symmetry positions for adsorbate atoms: the 4-coordinate oxygen pedestal (OP) and 2-coordinate oxygen bridge (OB) sites (figure 4(c)). Additionally, Al was placed at the high-symmetry sites of a (2 × 1) reconstructed O-terminated surface, which, while not stable for the clean surface, are stabilised by adsorbate addition. The procedure for addition of Al atoms for coverages above 0.25 ML was the same as described previously for (2 × 1) sites, and an analogous procedure was used for addition to the (1 × 1) surface.

Table 3 shows results for Al addition to the (2 × 1) reconstructed surface and whether this final configuration is obtained starting from addition to either ether or ketone O-terminated diamond. The minimum energy structures are shown in figure 5. Al bonds only weakly to the ether O-terminated surfaces, with the OB site lower in energy than OP. The only reconstruction observed is when the Al–Al bond is perpendicular to dimer rows at 0.5 ML coverage. The 1 ML surface is not stable.

In contrast to the ether-terminated surfaces, most configurations for the ketone O-termination relax into the (2 × 1) reconstructed surface. The weak ketone π-bond is broken by the presence of Al, but not the strong ether σ-bond. The 0.25 ML OP ketone configuration moves to the T3 position, and Al atoms at 0.5 ML coverage in OP positions relax into either the HH, HH + T3 (linear) or HH + T3 ($\sqrt{2} \times \sqrt{2}$) positions depending on the original arrangement. The HB site for <1 ML addition only causes reconstruction of the dimer above which it lies. At 1 ML, Al atoms in the ketone OP and OB positions move into the HH + T4 and HB + T4 positions, respectively, although in the case of HH + T4, the Al atoms in the HH sites are at different heights above the surface. The T3 site is the lowest energy site for both 0.25 and 0.5 ML

Table 2. Values of ionisation energy, I, electron affinity, χ, adsorption energy, E_{ads}, and relevant bond lengths, d, calculated for the minimum energy positions at different surface coverages of Al on the bare diamond surface. The HH and T3 sites at 0.25 ML coverage were not energy minima and so are not included.

Coverage (ML)	Structure	d(C–C) (Å)	d(C–Al) (Å)	I (eV)	χ (eV)	E_{ads} (eV)
0.25	HB	1.40, 1.75	2.00	5.43	−0.04	−3.11
0.25	T4	1.42, 1.70	2.11	5.02	−0.45	−3.60
0.50	HH	1.71	2.19	5.24	−0.23	−3.07
0.50	HB	1.84	2.02	5.10	−0.37	−3.56
0.50	T3	1.68	2.47	5.34	−0.13	−3.28
0.50	T4	1.63	2.18	4.54	−0.93	−3.97
0.50	HH + T3 (linear)	1.73	2.33, 2.32	5.51	0.04	−3.17
0.50	HB + T4 (linear)	1.45, 1.85	2.35, 2.19	5.30	−0.17	−3.73
0.50	HH + T3 ($\sqrt{2} \times \sqrt{2}$)	1.75	2.25, 2.49	5.50	0.03	−3.48
0.50	HB + T4 ($\sqrt{2} \times \sqrt{2}$)	1.65, 1.70	2.06, 2.13	5.28	−0.19	−3.56
1.00	HH + T3	1.65	2.08, 2.08	4.00	−1.47	−4.11
1.00	HH + T4	1.74	2.27, 2.74	4.54	−0.93	−3.83
1.00	HB + T3	1.69	2.12, 2.93	4.55	−0.92	−3.78
1.00	HB + T4	1.75	2.22, 2.27	4.92	−0.55	−3.87

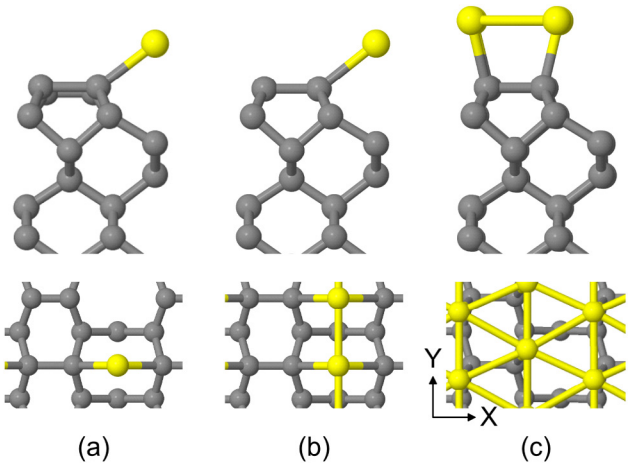

Figure 3. Minimum energy positions for (a)–(c) 0.25, 0.5 and 1 ML respectively of Al addition to the bare (1 0 0) diamond surface. Side and plan views are shown for each.

coverage, and for both it is formed by relaxation of the structure involving Al addition to the ketone O-terminated surface.

The clean ether and ketone surfaces have carbon–oxygen Mulliken bond populations of 0.57 and 1.21, respectively. After Al addition and subsequent relaxation into the sites shown in table 3, the C–O bonds have populations in the range 0.57–0.73, significantly closer to that for a single bond. For comparison, Al–O bond populations are in the range 0.1–0.43. Mulliken charges on Al are up to 2.16e, 1.58e and 1.08e at 0.25, 0.5 and 1 ML coverages, respectively. The preferred sites for adsorption in these cases are the more ionic HH and T3 sites at $<$1 ML coverage. However, in general, the 'covalent' sites have more negative EA than 'ionic' sites.

The electron affinity of the different Al-adsorbed O-terminated diamond surfaces are less negative than for addition to the bare surface, with more positions showing positive EA. Adsorption energies are larger than for addition to the bare surface. Increased coverage leads to decreased adsorption energies, the reverse of the trend observed for adsorption

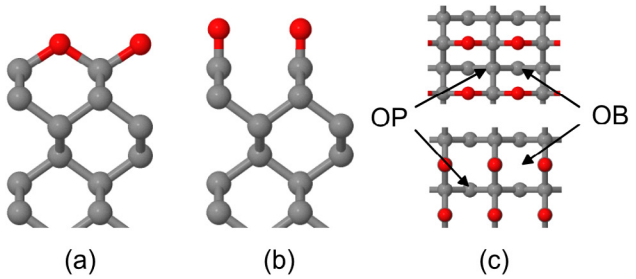

Figure 4. (a) Ether and (b) ketone arrangements of O-terminated diamond. (c) Plan view showing the two high-symmetry positions for adsorption on the O-terminated surface.

to the bare surface. This is technologically useful for better control of surface coverage and discouragement of island formation. The EA is less negative than observed by O'Donnell *et al* [20] for group I elements on O-terminated diamond, but adsorption energies are significantly higher. Compared with the transition metals studied by Tiwari *et al* [19], Al is most similar to Ti, with 0.25 ML coverage giving the largest NEA for both metals and comparable adsorption energies.

Electronic structure

Projected density-of-states (PDOS) were computed to study the effect of metal adsorption on electronic structure. In each case, the bulk valence band maximum is set to zero, and states originating from different sets of atoms are offset for clarity. Bulk carbon atoms are taken from the middle of the diamond slab and are not expected to change. The PDOS for surface carbon atoms are taken from the dimer row.

Figure 6 shows PDOS spectra for the clean oxygen-free and (ether) O-terminated diamond surfaces. The extra states within the band gap for the bare surface originate from π and $\pi*$ bonds of the dimer rows [23], and, similarly, O-termination also introduces inter-bandgap states from oxygen lone pairs [43].

Table 3. Values of ionisation energy, I, electron affinity, χ, adsorption energy, E_{ads}, and relevant bond lengths, d, calculated for the minimum energy positions at different surface coverages of Al on O-terminated diamond. $*$ indicates the particular (1×1) surface that forms this structure. (E) and (K) are ether and ketone configurations, respectively. The HB and T4 positions at 0.25 ML coverage and HB + T4 ($\sqrt{2} \times \sqrt{2}$) at 0.5 ML were not energy minima and so are not included.

Coverage (ML)	Structure	d(C–C) (Å)	d(C–O) (Å)	d(Al–O) (Å)	I (eV)	χ (eV)	E_{ads} (eV)
0.25	HH	1.70	1.36	1.82	4.11	−1.36	−5.24
0.25	T3 $*$OP (K)	1.63	1.36	1.78	5.10	−0.37	−6.36
0.50	HH $*$OP (E, K)	1.66	1.41	1.92	5.94	0.47	−5.61
0.50	HB $*$OB (K)	1.71	1.35	1.77	4.84	−0.63	−4.62
0.50	T3 $*$OB (K)	1.64	1.40	1.88	6.53	1.06	−5.99
0.50	T4	1.63	1.34	1.71	5.01	−0.46	−4.71
0.50	HH + T3 (linear) $*$OP (K)	1.64	1.40	1.85, 1.98	6.19	0.72	−5.85
0.50	HB + T4 (linear)	1.66	1.39	1.80, 1.88	5.78	0.31	−4.32
0.50	HH + T3 ($\sqrt{2} \times \sqrt{2}$) $*$OP (K)	1.65	1.40	1.88, 2.03	6.60	1.13	−5.85
1.00	HH + T3	1.65	1.40	1.92, 3.11	5.35	−0.12	−4.35
1.00	HH + T4 $*$OP (K)	1.66	1.39	1.88, 1.88, 1.99, 2.80	5.02	−0.45	−4.55
1.00	HB + T3	1.64	1.41	2.08, 2.09	6.01	0.54	−4.58
1.00	HB + T4 $*$OB (K)	1.64	1.39	1.84, 1.94	5.47	0.00	−4.35

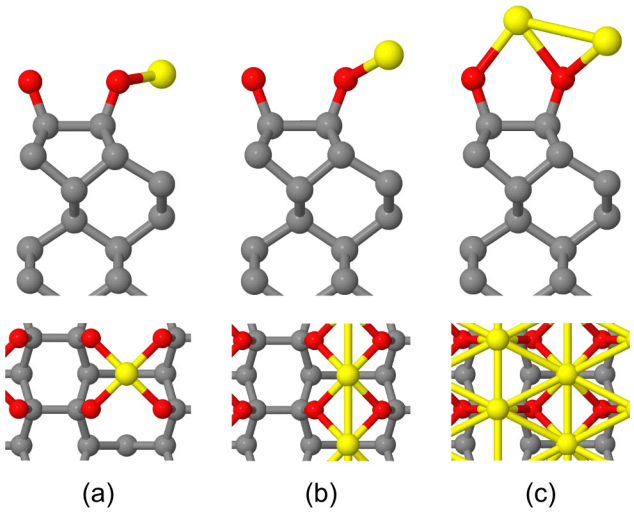

Figure 5. Minimum energy positions for (a)–(c) 0.25, 0.5 and 1 ML respectively of Al addition to the O-terminated (1 0 0) diamond surface. Side and plan views are shown for each.

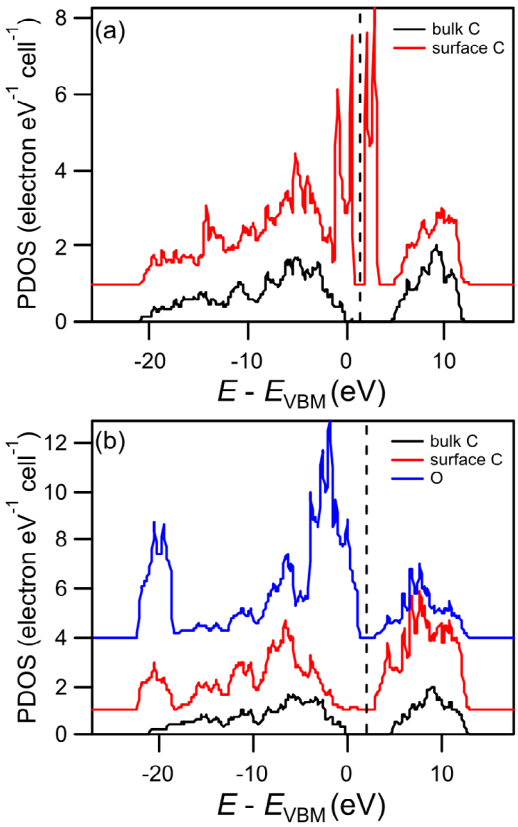

Figure 6. PDOS spectra evaluated for (a) bare surface and (b) O-terminated surface with ether configuration. The dashed vertical lines indicate the position of the Fermi level.

The PDOS spectra for the Al-adsorbed diamond surfaces are displayed in figure 7. These were computed for the lowest energy structures in tables 2 and 3. The bulk carbon PDOS spectra are similar in all cases, as expected. Starting with addition to the bare surface, all coverages show mixing of Al and surface C states indicating covalent bonding. At 0.25 ML coverage the broadness of the surface C DOS is due to there being two contributions to the DOS, as Al only interacts with one of the C dimers.

Turning to the PDOS for Al on the O-terminated surface, the aluminium DOS is considerably different from that of the bare surface due to the change from predominantly covalent to ionic bonding, consistent with the relative electronegativities of carbon and oxygen. The ionic bonding is most pronounced at 0.25 ML coverage where there are few occupied Al states near the valence band maximum. As the coverage increases, the 3*s* and 3*p* states of Al, unoccupied at 0.25 ML, move down in energy such that they become partially occupied. By 1 ML the Al DOS mixes with oxygen states indicating more covalent character; with increasing Al coverage the effective positive charge on each Al decreases due to the finite capacity for the oxygen atoms to accept negative charge. This combination of ionic and covalent behaviour, and the different co-ordinations of Al that are present are reflected by the complexity of the PDOS.

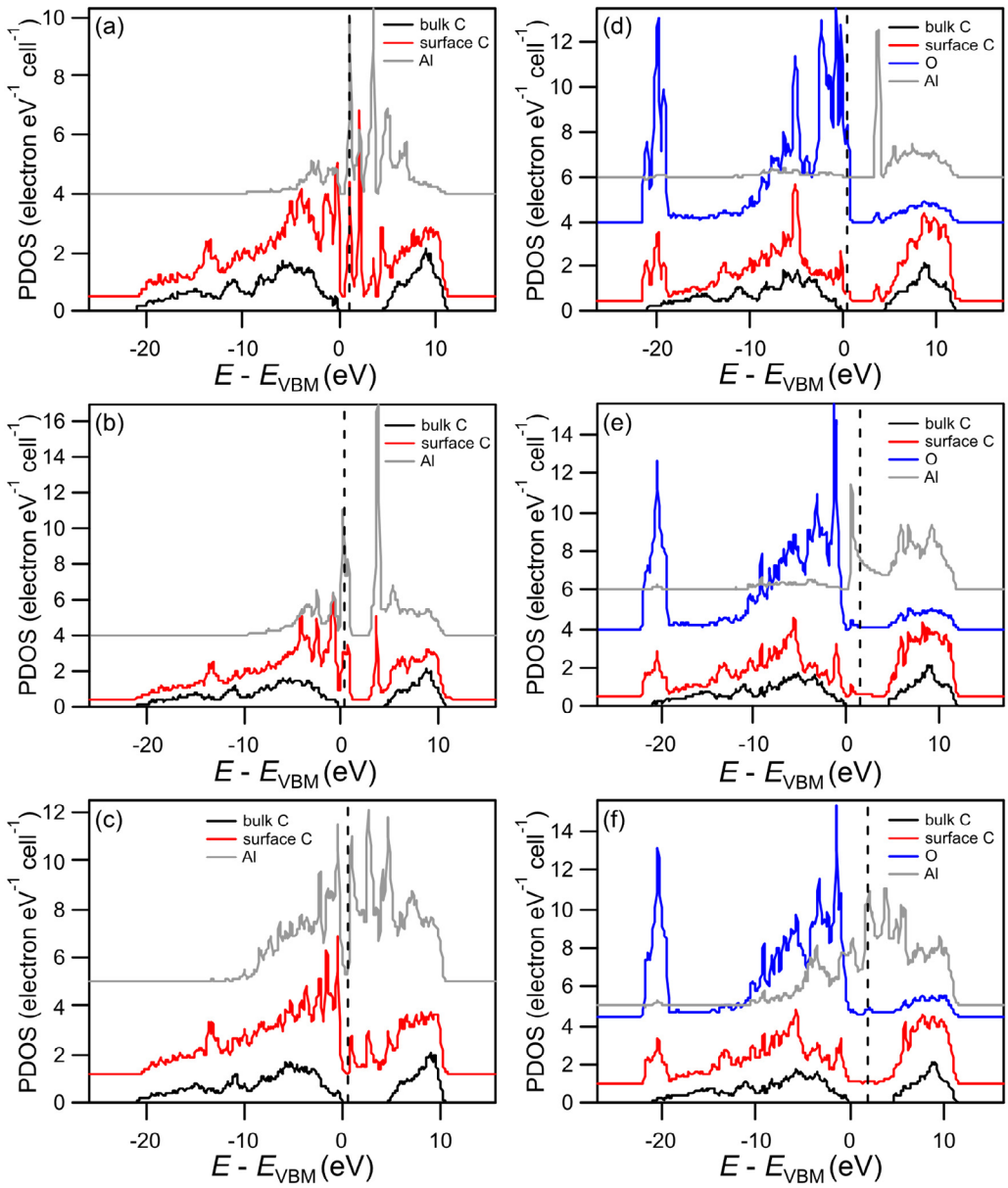

Figure 7. PDOS evaluated for (a)–(c) 0.25, 0.5 and 1 ML Al coverage on the bare diamond surface, and (d)–(f) 0.25, 0.5 and 1 ML Al coverage on the O-terminated surface. These are the lowest energy structures from tables 2 and 3. The dashed vertical lines indicate the highest occupied states.

Conclusions

DFT calculations were performed on the adsorption of Al onto the (1 0 0) bare and O-terminated diamond surfaces. A notable structural difference from previous studies of the adsorption of other metals at the bare diamond surface is that the preferred coordination number of Al to carbon is two, and the bonding at such sites is appreciably covalent in character. By contrast, on the O-terminated surface for <1 ML coverage, Al preferentially binds to sites where it is 4-coordinate and the bonding is more ionic. Al–Al interactions are important structurally at larger coverages. At 1 ML coverage, following relaxation of Al on the bare surface, a hexagonal arrangement of Al is lowest in energy, whilst for 1 ML coverage on the O-terminated surface, Al–Al interactions force some Al atoms further from the surface.

Al has relatively large adsorption energies of up to −4.11 and −6.36 eV on the bare and O-terminated surfaces, respectively. NEAs are possible for up to 1 ML coverage; however, control of atomic position is required as positive EA is shown in certain configurations. The magnitude of both NEA and adsorption energies for Al is most similar to that of Ti, a carbide-forming metal with comparable electronegativity. 0.25 ML coverage of Al on O-terminated diamond is predicted to have both NEA and stronger adsorption energies than H-terminated diamond regardless of adsorption site, and thus provides a possible route to a more temperature-stable surface termination. Work is currently underway to try and obtain an NEA value for Al on diamond experimentally.

Acknowledgments

This work was carried out using the computational facilities of the Advanced Computing Research Centre, University of Bristol—http://bris.ac.uk/acrc/. Structures were created using DL_VISUALIZE [44] and visualised using Jmol—http://jmol.org/. MCJ thanks the Engineering and Physical Sciences Research Council (EPSRC) for funding under grant code EP/L016648/1 as part of the Functional Nanomaterials CDT. Data are available at the University of Bristol data repository, data.bris, at https://doi.org/10.5523/bris.2fceiuzvtolvl2jd1ll285tzrz.

ORCID iDs

Michael C James https://orcid.org/0000-0002-0157-989X

References

[1] Monroy E, Omnès F and Calle F 2003 Wide-bandgap semiconductor ultraviolet photodetectors *Semicond. Sci. Technol.* **18** R33–51
[2] Ascarelli P, Cappelli E, Pinzari F, Rossi C, Salvatori S, Merli G and Migliori A 2001 Secondary electron emission from diamond: Physical modeling and application to scanning electron microscopy *J. Appl. Phys.* **89** 689–96
[3] Shih A, Yater J, Pehrsson P, Butler J, Hor C and Abrams R 1997 Secondary electron emission from diamond surfaces *J. Appl. Phys.* **82** 1860–7
[4] Koeck F A M, Nemanich R J, Lazea A and Haenen K 2009 Thermionic electron emission from low work-function phosphorus doped diamond films *Diam. Relat. Mater.* **18** 789–91
[5] Strobel P, Riedel M, Ristein J, Ley L and Boltalina O 2005 Surface transfer doping of diamond by fullerene *Diam. Relat. Mater.* **14** 451–8
[6] Van Der Weide J, Zhang Z, Baumann P K, Wensell M G, Bernholc J and Nemanich R J 1994 Negative-electron-affinity effects on the diamond (1 0 0) surface *Phys. Rev.* B **50** 5803–6
[7] Himpsel F J, Knapp J A, VanVechten J A and Eastman D E 1979 Quantum photoyield of diamond (1 1 1)—a stable negative-affinity emitter *Phys. Rev.* B **20** 624–7
[8] Baumann P K and Nemanich R J 1998 Surface cleaning, electronic states and electron affinity of diamond (1 0 0), (1 1 1) and (1 1 0) surfaces *Surf. Sci.* **409** 320–35
[9] Paxton W F, Howell M, Kang W P and Davidson J L 2012 Influence of hydrogen on the thermionic electron emission from nitrogen-incorporated polycrystalline diamond films *J. Vac. Sci. Technol.* B **30** 21202
[10] Loh K P, Foord J S, Egdell R G and Jackman R B 1997 Tuning the electron affinity of CVD diamond with adsorbed caesium and oxygen layers *Diam. Relat. Mater.* **5** 874–8
[11] Loh K P, Xie X N, Yang S W, Pan J S and Wu P 2002 A spectroscopic study of the negative electron affinity of cesium oxide-coated diamond (1 1 1) and theoretical calculation of the surface density-of-states on oxygenated diamond (1 1 1) *Diam. Relat. Mater.* **11** 1379–84
[12] Wong K W, Wang Y M, Lee S T and Kwok R W M 1999 Lowering of work function induced by deposition of ultra-thin rubidium fluoride layer on polycrystalline diamond surface *Appl. Surf. Sci.* **140** 144–9
[13] Nie J L, Xiao H Y and Zu X T 2006 First principles calculations on Na and K-adsorbed diamond (1 0 0) surface *Chem. Phys.* **326** 308–14
[14] Baumann P K and Nemanich R J 1996 Characterization of cobalt-diamond (1 0 0) interfaces: Electron affinity and Schottky barrier *Appl. Surf. Sci.* **104–5** 267–73
[15] Baumann P K and Nemanich R J 1998 Characterization of copper-diamond (1 0 0), (1 1 1), and (1 0 0) interfaces: electron affinity and Schottky barrier **58** 1643–54
[16] Baumann P K and Nemanich R J 1998 Electron affinity and Schottky barrier height of metal–diamond (1 0 0), (1 1 1), and (1 1 0) interfaces *J. Appl. Phys.* **83** 2072
[17] van der Weide J and Nemanich R J 1992 Schottky barrier height and negative electron affinity of titanium on (1 1 1) diamond *J. Vac. Sci. Technol.* B **10** 1940–3
[18] Tiwari A K, Goss J P, Briddon P R, Wright N G, Horsfall A B and Rayson M J 2012 Effect of different surface coverages of transition metals on the electronic and structural properties of diamond *Phys. Status Solidi* **209** 1697–702
[19] Tiwari A K, Goss J P, Briddon P R, Horsfall A B, Wright N G, Jones R and Rayson M J 2014 Unexpected change in the electron affinity of diamond caused by the ultra-thin transition metal oxide films *Europhys. Lett.* **108** 46005
[20] O'Donnell K M, Martin T L and Allan N L 2015 Light metals on oxygen-terminated diamond (1 0 0): structure and electronic properties *Chem. Mater.* **27** 1306–15
[21] O'Donnell K M, Martin T L, Edmonds M T, Tadich A, Thomsen L, Ristein J, Pakes C I, Fox N A and Ley L 2014 Photoelectron emission from lithiated diamond *Phys. Status Solidi* **211** 2209–22
[22] O'Donnell K M, Edmonds M T, Tadich A, Thomsen L, Stacey A, Schenk A, Pakes C I and Ley L 2015 Extremely high negative electron affinity of diamond via magnesium adsorption *Phys. Rev.* B **92** 35303
[23] Tiwari A K, Goss J P, Briddon P R, Wright N G, Horsfall A B and Rayson M J 2012 Electronic and structural properties of diamond (0 0 1) surfaces terminated by selected transition metals *Phys. Rev.* B **86** 155301
[24] Evans D A, Roberts O R, Vearey-Roberts A R, Langstaff D P, Twitchen D J and Schwitters M 2007 Direct observation of Schottky to Ohmic transition in Al-diamond contacts using real-time photoelectron spectroscopy *Appl. Phys. Lett.* **91** 132114
[25] Matsumoto T, Kato H, Oyama K, Makino T, Ogura M, Takeuchi D, Inokuma T, Tokuda N and Yamasaki S 2016 Inversion channel diamond metal-oxide-semiconductor field-effect transistor with normally off characteristics *Sci. Rep.* **6** 31585
[26] Maréchal A, Aoukar M, Vallée C, Rivière C, Eon D, Pernot J and Gheeraert E 2015 Energy-band diagram configuration of Al_2O_3/oxygen-terminated p-diamond metal-oxide-semiconductor *Appl. Phys. Lett.* **107** 1–5
[27] Hiraiwa A, Saito T, Matsumura D and Kawarada H 2015 Isotope analysis of diamond-surface passivation effect of high-temperature H_2O grown atomic layer deposition Al_2O_3 films *J. Appl. Phys.* **117** 215304
[28] Clark S J, Segall M D, Pickard C J, Hasnip P J, Probert M I J, Refson K and Payne M C 2005 First principles methods using CASTEP *Z. Krist.* **220** 567–70
[29] Perdew J P, Burke K and Ernzerhof M 1996 Generalized gradient approximation made simple *Phys. Rev. Lett.* **77** 3865–8
[30] Vanderbilt D 1990 Soft self-consistent pseudopotentials in a generalized eigenvalue formalism *Phys. Rev.* B **41** 7892–5
[31] Morris A J, Nicholls R J, Pickard C J and Yates J R 2014 OptaDOS: a tool for obtaining density of states, core-level and optical spectra from electronic structure codes *Comput. Phys. Commun.* **185** 1477–85

[32] Monkhorst H J and Pack J D 1976 Special points for Brillouin-zone integrations *Phys. Rev.* B **13** 5188–92
[33] Fall C J, Binggeli N and Baldereschi A 1999 Deriving accurate work functions from thin-slab calculations *J. Phys. Condens. Matter* **11** 2689–96
[34] O'Donnell K M, Martin T L, Fox N A and Cherns D 2010 *Ab initio* investigation of lithium on the diamond C(1 0 0) surface *Phys. Rev.* B **82** 115303
[35] Maier F, Ristein J and Ley L 2001 Electron affinity of plasma-hydrogenated and chemically oxidized diamond (1 0 0) surfaces *Phys. Rev.* B **64** 165411
[36] Furthmüller J, Hafner J and Kresse G 1994 Structural and electronic properties of clean and hydrogenated diamond (1 0 0) surfaces *Europhys. Lett.* **28** 659
[37] Rutter M J and Robertson J 1998 *Ab initio* calculation of electron affinities of diamond surfaces *Phys. Rev.* B **57** 9241–5
[38] Qi D, Liu L, Gao X, Ouyang T, Chen S, Loh K P and Wee A T S 2007 Tuning the electron affinity and secondary electron emission of diamond (1 0 0) surfaces by diels-alder reaction *Langmuir* **23** 9722–7
[39] Furthmüller J, Hafner J and Kresse G 1996 Surface reconstruction and electronic properties of clean and hydrogenated diamond (1 1 1) surfaces *Phys. Rev.* B **53** 7334–51
[40] Zheng X M and Smith P V 1992 The stable configurations for oxygen chemisorption on the diamond (1 0 0) and (1 1 1) surfaces *Surf. Sci.* **262** 219–34
[41] Tamura H *et al* 2000 Periodic density-functional study on oxidation of diamond (1 0 0) surfaces *Phys. Rev.* B **61** 11025–33
[42] Mulliken R S 1955 Electronic population analysis on LCAO-MO molecular wave functions. I *J. Chem. Phys.* **23** 1833–40
[43] Sque S J, Jones R and Briddon P R 2006 Structure, electronics, and interaction of hydrogen and oxygen on diamond surfaces *Phys. Rev.* B **73** 1–15
[44] Searle B G and Visualize D L 2001 *Comput. Phys. Commun.* **137** 25–32